

1 **A versatile pathway to end-functionalized cellulose ethers for click chemistry**  
2 **applications**

3

4 Hiroshi Kamitakahara<sup>\*</sup>, Ryo Suhara, Mao Yamagami, Haruko Kawano, Ryoko Okanishi, Tomoyuki  
5 Asahi, Toshiyuki Takano

6 Graduate School of Agriculture, Kyoto University, Sakyo-ku, Kyoto 606-8502, Japan

7 <sup>\*</sup>Corresponding author: [hkamitan@kais.kyoto-u.ac.jp](mailto:hkamitan@kais.kyoto-u.ac.jp)

8 Phone: +81-75-753-6257

9 Fax: +81-75-753-6300

10

11

## 12 **ABSTRACT**<sup>1</sup>

13 This paper describes a versatile pathway to heterobifunctional/telechelic cellulose ethers, such as  
14 tri-*O*-methyl cellulosyl azide and propargyl tri-*O*-methyl cellulose, having one free C-4 hydroxyl  
15 group attached to the glucosyl residue at the non-reducing end for the use in Huisgen 1,3-dipolar  
16 cycloaddition and copper(I)-catalyzed azide-alkyne cycloaddition (CuAAC). The one-step  
17 end-functionalization of cellulose ethers for molecular rod synthesis involves the introduction of  
18 two reactive groups at both ends of the cellulose molecule, and can afford linear triblock  
19 copolymers via CuAAC and further reactions. We were able to tailor the degree of polymerization  
20 of end-functionalized cellulose ethers with controlled amounts of a Lewis acid, namely SnCl<sub>4</sub>.  
21 Chemical structures of the above cellulose ethers and the reaction conditions for controlling  
22 molecular length are discussed.

23  
24 *Keywords:* end-functionalized cellulose ether; copper(I)-catalyzed azide-alkyne cycloaddition;  
25 functional molecular rod; tri-*O*-methyl cellulosyl azide; propargyl tri-*O*-methyl cellulose

## 26 27 **1. Introduction**

28 Methylcellulose (MC), being one of the more common cellulose ethers, has been of interest in the  
29 investigation of structure-property relationships, such as thermoreversible gelation properties at  
30 elevated temperature. Our research focuses on the design and synthesis of regioselectively  
31 methylated cellulose derivatives via ring-opening polymerization of glucose ortho-pivalate  
32 derivatives (Kamitakahara, Hori, & Nakatsubo, 1996; Karakawa, Mikawa, Kamitakahara, &  
33 Nakatsubo, 2002; Nakatsubo, Kamitakahara, & Hori, 1996) or from natural cellulose  
34 (Kamitakahara, Koschella, Mikawa, Nakatsubo, Heinze, & Klemm, 2008; Nakagawa et al., 2012)  
35 and diblock methylcellulose with regioselective functionalization patterns (Nakagawa, Fenn,  
36 Koschella, Heinze, & Kamitakahara, 2011a, b; Nakagawa, Steiniger, Richter, Koschella, Heinze, &  
37 Kamitakahara, 2012). As a result, we found that a diblock structure composed of hydrophilic  
38 cellobiosyl and hydrophobic 2,3,6-tri-*O*-methylcellulosyl segments is crucial for the  
39 thermoreversible gelation of aqueous MC solutions (Nakagawa, Fenn, Koschella, Heinze,  
40 Kamitakahara, 2011a). Commercial MC prepared under heterogeneous conditions is an  
41 alternating block copolymer composed of densely substituted hydrophobic and less densely  
42 substituted hydrophilic block sequences (Savage, 1957). The synthetic route to multiblock MC  
43 derivatives composed of hydrophobic 2,3,6-tri-*O*-methylcellulosyl and hydrophilic cellulose  
44 segments remains open.

---

<sup>1</sup> Copper(I)-catalyzed azide-alkyne cycloaddition, CuAAC; methylcellulose, MC; cellulose triacetate, CTA; gel permeation chromatography, GPC; 2,5-dihydroxybenzoic acid, DHB; degree of polymerization, DP.

45

46 Precise control of the monosaccharide sequence to prepare multiblock derivatives is, however,  
47 extremely difficult and time-consuming. We synthesized 1,2,3-triazole-linked diblock MC  
48 composed of low molecular weight cellulose and 2,3,6-tri-*O*-methyl cellulose (Nakagawa,  
49 Kamitakahara, & Takano, 2012) and found that a 2 wt. % aqueous solution of this MC analogue  
50 exhibited thermoreversible gelation behavior, meaning that linkages between hydrophilic and  
51 hydrophobic segments do not affect gelation properties. Thus, we considered utilizing linkages  
52 other than the glycosidic bond to prepare multiblock MC copolymers.

53

54 To be suitable building blocks for the multiblock MC copolymers, the cellulose derivatives must  
55 have functional groups at both ends of the linear molecule. Heterobifunctional/telechelic  
56 derivatives are more desirable than homobifunctional/telechelic ones (Kim, Stannett, & Gilbert,  
57 1973, 1976; Pohjola & Eklund, 1977; Steinmann, 1968, 1970) for the preparation of multiblock  
58 copolymers. Derivatives having two different functional groups at both ends of the linear polymer  
59 are therefore attractive and promising for the exploration of a new research field in cellulose  
60 chemistry.

61

62 On the other hand, cellulose derivatives are known to be semi-rigid polymers (De Oliveira &  
63 Glasser, 1994), which controls their physical properties. The concept of a 'molecular rod' is  
64 therefore applicable to heterobifunctional/telechelic cellulose derivatives, which can be viewed as  
65 bricks of a molecular Lego (Lepage, Schneider, Bodlener, & Compain, 2015; Meldal, 2008). To  
66 connect several bricks of the cellulosic Lego, two ends of the molecular rod must be separately  
67 functionalized under independent activation conditions. It is then possible to covalently bind  
68 several molecular bricks, adding other brick units under different reaction conditions.

69

70 We have previously reported the synthesis of tri-*O*-acetyl cellulosyl azide (Kamitakahara, Enomoto,  
71 Hasegawa, & Nakatsubo, 2005). This molecule is a key compound for the end-functionalization  
72 of cellulose derivatives. The azide group can be easily converted into an amino group, which can  
73 be used in a subsequent amidation reaction. For instance, we successfully synthesized cellulose  
74 triacetate (CTA)-*block*-oligoamide-15 (Kamitakahara, Enomoto, Hasegawa, & Nakatsubo, 2005;  
75 Kamitakahara & Nakatsubo, 2005), a CTA derivative carrying a single pyrene group at the reducing  
76 end (Enomoto, Kamitakahara, Takano, & Nakatsubo, 2006), and a CTA derivative having a single  
77 lipoic acid moiety at the reducing end (Enomoto-Rogers, Kamitakahara, Yoshinaga, & Takano,  
78 2010). The high reactivity of the azide group towards alkynes is known as the click chemistry  
79 approach, and is based on Huisgen 1,3-dipolar cycloaddition and copper(I)-catalyzed azide-alkyne  
80 cycloaddition (CuAAC) (Kolb, Finn, & Sharpless, 2001). We have prepared comb-shaped graft

81 copolymers with CTA side chains (Enomoto-Rogers, Kamitakahara, Yoshinaga, & Takano, 2012)  
82 and CTA-block-poly( $\gamma$ -benzyl-L-glutamate) (Kamitakahara, Baba, Yoshinaga, Suhara, & Takano,  
83 2014), knowing that the CuAAC reaction is a more powerful tool for bonding two polymeric  
84 segments than amidation.

85

86 Not only cellulose esters, such as cellulose acetate, but also a representative cellulose ether,  
87 methylcellulose, were also important molecular Lego bricks. Methyl tri-*O*-methyl cellulose, with  
88 a single hydroxyl group at the C-4 position of the glucosyl residue at the non-reducing end was  
89 prepared by methanolysis of 2,3,6-tri-*O*-methyl cellulose (Nakagawa, Fenn, Koschella, Heinze, &  
90 Kamitakahara, 2011b; Nakagawa, Kamitakahara, & Takano, 2011). Propargylation of one end of  
91 the cellulose ether derivative afforded a cellulose ether carrying a single alkyne group at the end of  
92 the cellulosic molecular rod, methyl tri-*O*-methyl cellulose (Nakagawa, Kamitakahara, & Takano,  
93 2012). Cellulose ethers are more stable than the corresponding esters in both acidic and alkaline  
94 reaction conditions used to construct the cellulosic molecular architecture. Thus, we focused on  
95 the synthesis of cellulosic molecular rods carrying two independent end-functional groups.

96

97 Propargylated methyl tri-*O*-methyl cellulose was synthesized from commercial methylcellulose in  
98 three reaction steps: complete methylation, methanolysis, and propargylation. This molecular rod  
99 has a functional group at one end (Nakagawa, Fenn, Koschella, Heinze, & Kamitakahara, 2011b),  
100 which is a disadvantage. Therefore, we were motivated to synthesize cellulosic molecular rods  
101 carrying two independent end-functional groups, in other words, cellulosic  
102 heterobifunctional/telechelic polymers.

103

104 To introduce an azide group at the C-1 position of the glucosyl residue at the reducing end of CTA,  
105 it was treated with hydrogen bromide in acetic acid to afford the  $\alpha$ -anomer of tri-*O*-acetyl cellulose  
106 bromide. The bromide was then treated with acetic acid and silver oxide to yield the  $\beta$ -anomer of  
107 acetyl tri-*O*-acetyl cellulose, which was finally converted into the  $\beta$ -anomer of tri-*O*-acetyl  
108 cellulose azide using trimethylsilyl azide and SnCl<sub>4</sub> (Kamitakahara, Enomoto, Hasegawa, &  
109 Nakatsubo, 2005). We tried to produce tri-*O*-methyl cellulose azide (**2**) with a controlled  
110 molecular weight from tri-*O*-methyl cellulose (**1**) in a one-step reaction. Azide and alkyne groups  
111 form a pair for the 1,3-dipolar cycloaddition, and preparing propargyl tri-*O*-methyl cellulose (**3**) is,  
112 therefore, of critical importance. Thus, we attempted to produce propargyl tri-*O*-methyl cellulose  
113 (**3**) with a controlled molecular weight from tri-*O*-methyl cellulose (**1**) in a one-step reaction.

114

115 Moreover, the free C-4 hydroxyl of the glucosyl residue at the non-reducing end could connect with  
116 other molecular bricks having epoxide, acyl, isocyanate, and other functionalities, thereby

117 extending the variety of molecular architecture motifs. Heterobifunctional/telechelic cellulose  
118 derivatives, at least, provide molecules with triblock structures. The production of cellulosic  
119 triblock copolymers from homobifunctional/telechelic cellulose derivatives has already been  
120 reported (Kim, Stannett, & Gilbert, 1973, 1976; Pohjola & Eklund, 1977; Steinmann, 1968, 1970),  
121 however, heterobifunctional/telechelic cellulose derivatives are still unknown, to the best of our  
122 knowledge.

123

124 Consequently, the aim of this research was to find the appropriate reaction conditions affording  
125 end-functionalized cellulose ethers, such as tri-*O*-methyl cellulose azide (**2**) and propargyl  
126 tri-*O*-methyl cellulose (**3**), for click chemistry and further conversion using the remaining  
127 functionalized end of the ethers. This paper describes well-controlled synthetic methods for  
128 preparing cellulosic precursors for CuAAC, namely tri-*O*-methyl cellulose azide (**2**) and propargyl  
129 tri-*O*-methyl cellulose (**3**). The reaction conditions used to introduce azide and propargyl groups  
130 onto the tri-*O*-methyl cellulose (**1**) scaffold and the structures of reaction products are also  
131 discussed.

132

## 133 **2. MATERIALS AND METHODS**

### 134 **2.1. Materials**

135 All reagents and solvents were obtained from Nacalai Tesque, Wako Chemical, and Sasaki  
136 Chemical, Japan, and were used as received.

137

### 138 **2.2. Analytical measurements**

139 <sup>1</sup>H and <sup>13</sup>C NMR spectra were acquired in CDCl<sub>3</sub> on a Varian 500 NMR spectrometer at room  
140 temperature. The molecular weights of the products were measured by gel permeation  
141 chromatography (GPC) in chloroform on a Shimadzu SEC system (CBM-20A, SPD-10A<sub>VP</sub>,  
142 SIL-10A, LC-10AT<sub>VP</sub>, FCV-10AL<sub>VP</sub>, CTO-10A<sub>VP</sub>, RID-10A, and FRC-10A, Shimadzu, Japan).  
143 Sample solutions were passed through a syringe filter (Sartorius Stedim, Minisart RC 4 or RC 15;  
144 pore size 0.45 μm) before GPC analysis. Shodex columns (K802, K802.5, and K805) with a  
145 guard column (Shodex, K-G) were used. Number- and weight-averaged molecular weights ( $M_n$   
146 and  $M_w$ ) and polydispersity indices ( $M_w/M_n$ ) were estimated using polystyrene standards (Shodex).  
147 Matrix-assisted laser desorption/ionization time-of-flight mass spectra (MALDI-TOF MS) were  
148 recorded on a Bruker Autoflex III machine in the positive ion linear mode. 2,5-Dihydroxybenzoic  
149 acid (DHB) was used as a matrix for these measurements.

150

### 151 **2.3. Synthetic methods**

#### 152 **2.3.1. 2,3,6-Tri-*O*-methyl cellulose (**1**)**

153 Complete methylation of SM-400 (Shin-Etsu Chemical, Japan) to afford 2,3,6-tri-*O*-methyl  
154 cellulose (**1**) was carried out as previously described (Nakagawa, Kamitakahara, & Takano, 2011).  
155 MALDI-TOF MS (positive linear mode; DHB matrix):  
156 DP (degree of polymerization) = 5: C<sub>47</sub>H<sub>86</sub>O<sub>26</sub> Calcd. [M]<sup>+</sup> 1066.54; Found [M+Na]<sup>+</sup> = 1089.637  
157 DP = 6: C<sub>56</sub>H<sub>102</sub>O<sub>31</sub> Calcd. [M]<sup>+</sup> 1270.64; Found [M+Na]<sup>+</sup> = 1293.733  
158 DP = 7: C<sub>65</sub>H<sub>118</sub>O<sub>36</sub> Calcd. [M]<sup>+</sup> 1474.74; Found [M+Na]<sup>+</sup> = 1497.964  
159 DP = 8: C<sub>74</sub>H<sub>134</sub>O<sub>41</sub> Calcd. [M]<sup>+</sup> 1678.84; Found [M+Na]<sup>+</sup> = 1701.954  
160 DP = 9: C<sub>83</sub>H<sub>150</sub>O<sub>46</sub> Calcd. [M]<sup>+</sup> 1882.94; Found [M+Na]<sup>+</sup> = 1905.979  
161 DP = 10: C<sub>92</sub>H<sub>166</sub>O<sub>51</sub> Calcd. [M]<sup>+</sup> 2087.04; Found [M+Na]<sup>+</sup> = 2109.946  
162 DP = 11: C<sub>101</sub>H<sub>182</sub>O<sub>56</sub> Calcd. [M]<sup>+</sup> 2291.14; Found [M+Na]<sup>+</sup> = 2313.76  
163 DP = 12: C<sub>110</sub>H<sub>198</sub>O<sub>61</sub> Calcd. [M]<sup>+</sup> 2495.24; Found [M+Na]<sup>+</sup> = 2517.776  
164 DP = 13: C<sub>119</sub>H<sub>214</sub>O<sub>66</sub> Calcd. [M]<sup>+</sup> 2699.34; Found [M+Na]<sup>+</sup> = 2721.576  
165 DP = 14: C<sub>128</sub>H<sub>230</sub>O<sub>71</sub> Calcd. [M]<sup>+</sup> 2903.44; Found [M+Na]<sup>+</sup> = 2926.146  
166 DP = 15: C<sub>137</sub>H<sub>246</sub>O<sub>76</sub> Calcd. [M]<sup>+</sup> 3107.54; Found [M+Na]<sup>+</sup> = 3129.431  
167 DP = 16: C<sub>146</sub>H<sub>262</sub>O<sub>81</sub> Calcd. [M]<sup>+</sup> 3311.64; Found [M+Na]<sup>+</sup> = 3332.968  
168 DP = 17: C<sub>155</sub>H<sub>278</sub>O<sub>86</sub> Calcd. [M]<sup>+</sup> 3515.74; Found [M+Na]<sup>+</sup> = 3536.968  
169 DP = 18: C<sub>164</sub>H<sub>294</sub>O<sub>91</sub> Calcd. [M]<sup>+</sup> 3717.84; Found [M+Na]<sup>+</sup> = 3740.437  
170 DP = 19: C<sub>173</sub>H<sub>310</sub>O<sub>96</sub> Calcd. [M]<sup>+</sup> 3923.94; Found [M+Na]<sup>+</sup> = 3944.958

171

### 172 2.3.2. Tri-*O*-methyl cellulosyl azide (**2**)

173 To a solution of tri-*O*-methyl cellulose (**1**) (51.1 mg,  $M_n = 2.58 \times 10^{-4}$ ,  $DP_n = 126$ ) in anhydrous  
174 chloroform (0.633 mL) were added 0.32 mL of trimethylsilyl azide (0.2 mL) in anhydrous  
175 chloroform (9.8 mL) (TMS-N<sub>3</sub>:  $4.87 \times 10^{-2}$  mmol, 0.195 equiv./anhydro glucose unit (AGU)) and  
176 0.047 mL of tin(IV) tetrachloride (0.1 mL) in anhydrous chloroform (4.9 mL) (SnCl<sub>4</sub>:  $8.16 \times 10^{-3}$   
177 mmol, 0.034 equiv./AGU). The reaction mixture was stirred at room temperature (r.t.) for 4 h and  
178 was subsequently neutralized with 0.113 mL of triethylamine (0.2 mL) in chloroform (9.8 mL)  
179 (Et<sub>3</sub>N: 2 equiv. with respect to SnCl<sub>4</sub>). The reaction mixture was extracted with ethyl acetate,  
180 washed with water and brine, dried over Na<sub>2</sub>SO<sub>4</sub>, and concentrated *in vacuo* to give tri-*O*-methyl  
181 cellulosyl azide (**2**) (42.6 mg).

182 <sup>1</sup>H-NMR (500 MHz, CDCl<sub>3</sub>): δ 2.96 (t,  $J = 9.0$  Hz, H2), 3.22 (t,  $J = 9.0$  Hz, H3), 3.29 (broad d,  $J =$   
183 9.0 Hz, H5), 3.39 (OCH<sub>3</sub>), 3.54 (OCH<sub>3</sub>), 3.58 (OCH<sub>3</sub>), 3.62–3.84 (H4, H6), 4.28 (d,  $J = 8.0$ , H1),  
184 4.34 (d,  $J = 8.0$ , internal H1), 4.47 (d,  $J = 8.5$  Hz, H1-β at reducing end), 5.45 (d,  $J = 3.5$  Hz, H1-α  
185 at reducing end).

186 <sup>13</sup>C-NMR (125 MHz, CDCl<sub>3</sub>): δ 59.0, 59.1, 59.1 (C6-OCH<sub>3</sub>), 59.2, 59.4, 60.1, 60.3 (C3-OCH<sub>3</sub>),  
187 60.4, 60.5 (C2-OCH<sub>3</sub>), 60.6, 60.7, 60.8, 61.3, 69.8, 69.9, 70.2 (C6 internal), 70.5, 71.0, 72.3, 74.8  
188 (C5 internal), 74.9, 75.7, 76.9, 77.2, 77.4 (C4 internal), 77.5, 80.8, 81.1, 81.2, 82.8, 83.1, 83.4, 83.5

189 (C2 internal), 84.6, 84.9, 85.0 (C3 internal), 85.1, 87.0 (C1 $\alpha$  at reducing end), 87.3, 89.9 (C1 $\beta$  at  
190 reducing end), 103.1 (C1 internal), 103.3, 103.4.

191 MALDI-TOF MS (positive linear mode; DHB matrix):

192 DP = 5: C<sub>45</sub>H<sub>81</sub>N<sub>3</sub>O<sub>25</sub> Calcd. [M]<sup>+</sup> 1063.52; Found [M+Na]<sup>+</sup> = 1086.441

193 DP = 6: C<sub>54</sub>H<sub>97</sub>N<sub>3</sub>O<sub>30</sub> Calcd. [M]<sup>+</sup> 1267.62; Found [M+Na]<sup>+</sup> = 1290.637

194 DP = 7: C<sub>63</sub>H<sub>113</sub>N<sub>3</sub>O<sub>35</sub> Calcd. [M]<sup>+</sup> 1471.72; Found [M+Na]<sup>+</sup> = 1494.81

195 DP = 8: C<sub>72</sub>H<sub>129</sub>N<sub>3</sub>O<sub>40</sub> Calcd. [M]<sup>+</sup> 1675.82; Found [M+Na]<sup>+</sup> = 1698.909

196 DP = 9: C<sub>81</sub>H<sub>145</sub>N<sub>3</sub>O<sub>45</sub> Calcd. [M]<sup>+</sup> 1879.92; Found [M+Na]<sup>+</sup> = 1902.891

197 DP = 10: C<sub>90</sub>H<sub>161</sub>N<sub>3</sub>O<sub>50</sub> Calcd. [M]<sup>+</sup> 2084.01; Found [M-N<sub>2</sub>+Na]<sup>+</sup> = 2078.970, [M-N<sub>2</sub>+K]<sup>+</sup> =

198 2094.96, [M+Na]<sup>+</sup> = 2106.909, [M+K]<sup>+</sup> = 2122.97

199 DP = 11: C<sub>99</sub>H<sub>177</sub>N<sub>3</sub>O<sub>55</sub> Calcd. [M]<sup>+</sup> 2288.11; Found [M+Na]<sup>+</sup> = 2310.949

200 DP = 12: C<sub>108</sub>H<sub>193</sub>N<sub>3</sub>O<sub>60</sub> Calcd. [M]<sup>+</sup> 2492.21; Found [M+Na]<sup>+</sup> = 2515.075

201 DP = 13: C<sub>117</sub>H<sub>209</sub>N<sub>3</sub>O<sub>65</sub> Calcd. [M]<sup>+</sup> 2696.31; Found [M+Na]<sup>+</sup> = 2718.929

202 DP = 14: C<sub>126</sub>H<sub>225</sub>N<sub>3</sub>O<sub>70</sub> Calcd. [M]<sup>+</sup> 2900.41; Found [M+Na]<sup>+</sup> = 2922.819

203 DP = 15: C<sub>135</sub>H<sub>241</sub>N<sub>3</sub>O<sub>75</sub> Calcd. [M]<sup>+</sup> 3104.51; Found [M+Na]<sup>+</sup> = 3126.248

204 DP = 16: C<sub>144</sub>H<sub>257</sub>N<sub>3</sub>O<sub>80</sub> Calcd. [M]<sup>+</sup> 3308.61; Found [M+Na]<sup>+</sup> = 3331.014

205 DP = 17: C<sub>153</sub>H<sub>273</sub>N<sub>3</sub>O<sub>85</sub> Calcd. [M]<sup>+</sup> 3512.71; Found [M+Na]<sup>+</sup> = 3534.132

206 DP = 18: C<sub>162</sub>H<sub>289</sub>N<sub>3</sub>O<sub>90</sub> Calcd. [M]<sup>+</sup> 3716.81; Found [M+Na]<sup>+</sup> = 3738.273

207 DP = 19: C<sub>171</sub>H<sub>305</sub>N<sub>3</sub>O<sub>95</sub> Calcd. [M]<sup>+</sup> 3920.91; Found [M+Na]<sup>+</sup> = 3942.31.

208

### 209 2.3.3. Propargyl tri-*O*-methyl cellulose (**3**)

210 To a solution of tri-*O*-methyl cellulose (**1**) (50 mg,  $M_n = 2.58 \times 10^{-4}$ ,  $DP_n = 126$ ) in anhydrous  
211 dichloromethane (1 mL) were added 2-propyne-1-ol (4.2  $\mu$ L,  $7.1 \times 10^{-2}$  mmol, 0.3 equiv./AGU) and  
212 SnCl<sub>4</sub> (2.4  $\mu$ L, 0.021 mmol, 0.085 equiv./AGU). The reaction mixture was stirred at r.t. for 4 h  
213 and was subsequently extracted with chloroform, washed with water and brine, dried over Na<sub>2</sub>SO<sub>4</sub>,  
214 and concentrated *in vacuo* to give propargyl tri-*O*-methyl cellulose (**3**) (42 mg).

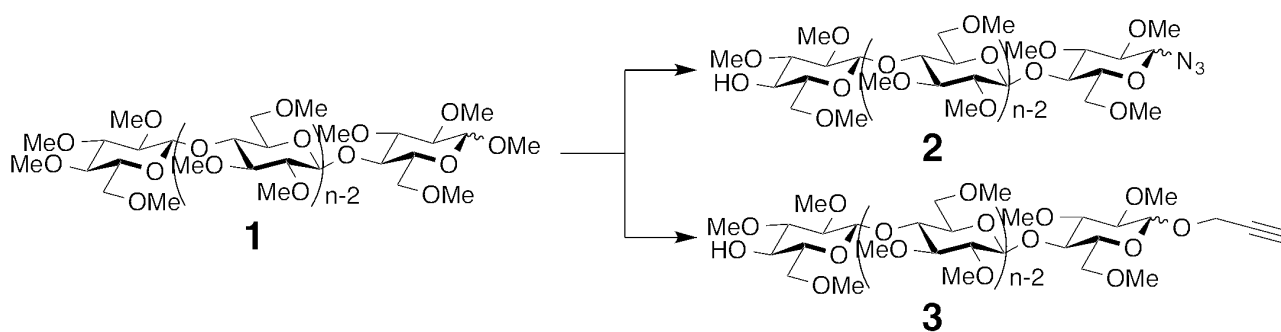
215 <sup>1</sup>H-NMR (500 MHz, CDCl<sub>3</sub>):  $\delta$  2.43 (CH<sub>2</sub>CCH), 2.95 (t,  $J = 9.0$  Hz, H2), 3.20 (t,  $J = 9.0$  Hz, H3)  
216 3.28 (broad d,  $J = 9.0$  Hz, H5), 3.37(OCH<sub>3</sub>), 3.53(OCH<sub>3</sub>), 3.57 (OCH<sub>3</sub>), 3.62–3.66 (H6), 3.72–3.81  
217 (H6), 3.69 (t,  $J = 9.0$  Hz, H4), 4.28–4.29 (CH<sub>2</sub>CCH), 4.34 (d, 1H,  $J = 8.0$ , internal H1), 4.38–4.39  
218 (CH<sub>2</sub>CCH), 4.49 (d,  $J = 8.0$  Hz, H1- $\beta$  at reducing end), 5.20 (d,  $J = 4.0$  Hz, H1- $\alpha$  at reducing end).

219 <sup>13</sup>C-NMR (125 MHz, CDCl<sub>3</sub>):  $\delta$  54.4 (CH<sub>2</sub>CCH (C1- $\alpha$ )), 55.6 (CH<sub>2</sub>CCH (C1- $\beta$ )), 58.4, 59.0, 59.1  
220 (C6-OCH<sub>3</sub>), 59.2, 59.3, 59.6, 60.1, 60.3 (C3-OCH<sub>3</sub>), 60.3, 60.4, 60.5 (C2-OCH<sub>3</sub>), 60.7, 60.8, 70.0,  
221 70.2 (C6 (internal)), 70.4, 72.0, 73.1, 73.3, 74.6, 74.7, 74.8 (C5 internal), 74.9, 77.1, 77.2, 77.4 (C4  
222 internal), 77.5, 77.6, 77.9, 78.7, 78.9, 79.3, 80.7, 81.0, 82.8 (C2 at reducing end (C1- $\beta$ )), 83.3, 83.5  
223 (C2 internal), 83.7, 84.4 (C3 at reducing end (C1- $\beta$ )), 84.9, 85.0 (C3 internal), 86.1, 94.5 (C1- $\alpha$  at  
224 reducing end), 100.7 (C1- $\beta$  at reducing end), 101.2, 103.1 (C1 internal), 103.2, 103.3.

225 MALDI-TOF MS (positive linear mode; DHB as matrix):  
 226 DP = 4: C<sub>39</sub>H<sub>68</sub>O<sub>21</sub> Calcd. [M]<sup>+</sup> 872.43; Found [M+Na]<sup>+</sup> = 895.164  
 227 DP = 5: C<sub>48</sub>H<sub>84</sub>O<sub>26</sub> Calcd. [M]<sup>+</sup> 1076.53; Found [M+Na]<sup>+</sup> = 1099.249  
 228 DP = 6: C<sub>57</sub>H<sub>100</sub>O<sub>31</sub> Calcd. [M]<sup>+</sup> 1280.62; Found [M+Na]<sup>+</sup> = 1303.425  
 229 DP = 7: C<sub>66</sub>H<sub>116</sub>O<sub>36</sub> Calcd. [M]<sup>+</sup> 1484.72; Found [M+Na]<sup>+</sup> = 1507.497  
 230 DP = 8: C<sub>75</sub>H<sub>132</sub>O<sub>41</sub> Calcd. [M]<sup>+</sup> 1688.82; Found [M+Na]<sup>+</sup> = 1711.584  
 231 DP = 9: C<sub>84</sub>H<sub>148</sub>O<sub>46</sub> Calcd. [M]<sup>+</sup> 1892.92; Found [M+Na]<sup>+</sup> = 1915.701  
 232 DP = 10: C<sub>93</sub>H<sub>164</sub>O<sub>51</sub> Calcd. [M]<sup>+</sup> 2097.02; Found [M+Na]<sup>+</sup> = 2119.702  
 233 DP = 11: C<sub>102</sub>H<sub>180</sub>O<sub>56</sub> Calcd. [M]<sup>+</sup> 2301.12; Found [M+Na]<sup>+</sup> = 2323.797  
 234 DP = 12: C<sub>111</sub>H<sub>196</sub>O<sub>61</sub> Calcd. [M]<sup>+</sup> 2505.22; Found [M+Na]<sup>+</sup> = 2527.612  
 235 DP = 13: C<sub>120</sub>H<sub>212</sub>O<sub>66</sub> Calcd. [M]<sup>+</sup> 2709.32; Found [M+Na]<sup>+</sup> = 2731.001  
 236 DP = 14: C<sub>129</sub>H<sub>228</sub>O<sub>71</sub> Calcd. [M]<sup>+</sup> 2913.42; Found [M+Na]<sup>+</sup> = 2936.027  
 237 DP = 15: C<sub>138</sub>H<sub>244</sub>O<sub>76</sub> Calcd. [M]<sup>+</sup> 3117.52; Found [M+Na]<sup>+</sup> = 3139.696  
 238 DP = 16: C<sub>147</sub>H<sub>260</sub>O<sub>81</sub> Calcd. [M]<sup>+</sup> 3321.62; Found [M+Na]<sup>+</sup> = 3343.723  
 239 DP = 17: C<sub>156</sub>H<sub>276</sub>O<sub>86</sub> Calcd. [M]<sup>+</sup> 3525.72; Found [M+Na]<sup>+</sup> = 3547.69  
 240 DP = 18: C<sub>165</sub>H<sub>292</sub>O<sub>91</sub> Calcd. [M]<sup>+</sup> 3729.82; Found [M+Na]<sup>+</sup> = 3752.824  
 241 DP = 19: C<sub>174</sub>H<sub>308</sub>O<sub>96</sub> Calcd. [M]<sup>+</sup> 3933.92; Found [M+Na]<sup>+</sup> = 3956.686.

242

### 243 3. Results and Discussion



244

245 **Scheme 1.** Synthesis of tri-*O*-methyl cellulose azide (**2**) and propargyl tri-*O*-methyl celluloside (**3**)  
 246 from tri-*O*-methyl cellulose (**1**).

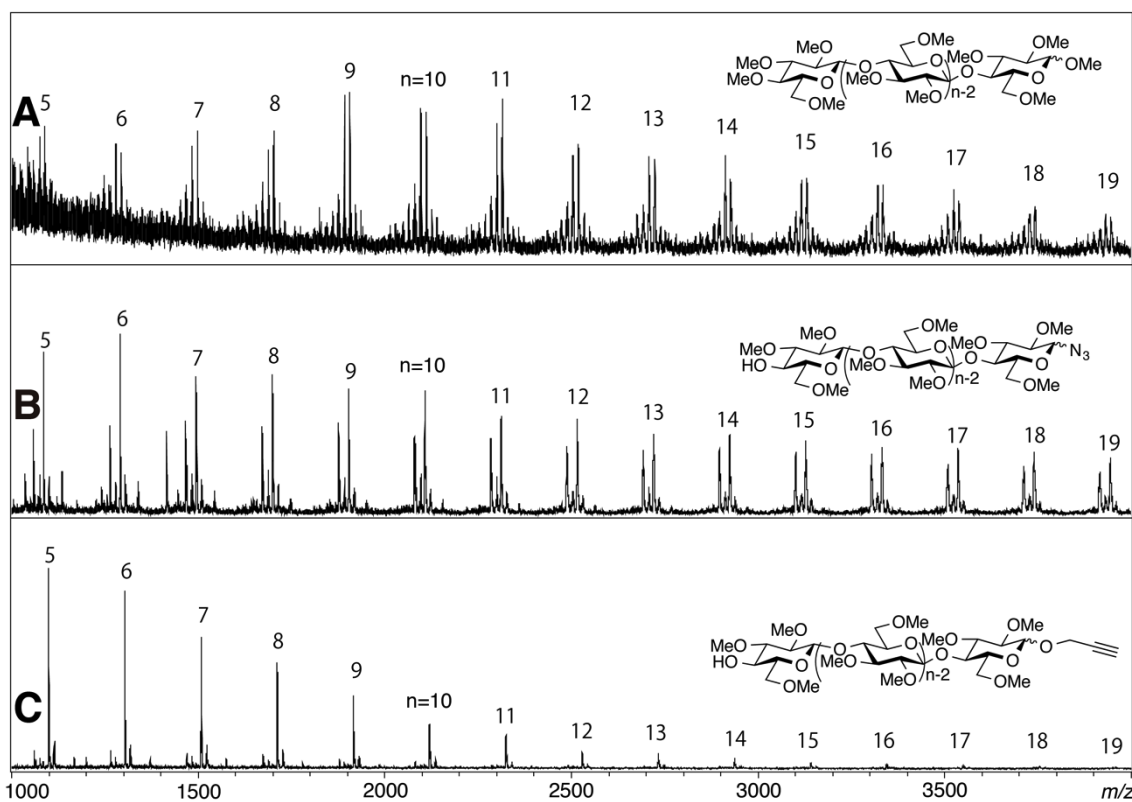
247

#### 248 3.1. Tri-*O*-methyl cellulose (**1**)

249 The MALDI-TOF MS spectrum of tri-*O*-methyl cellulose (**1**) (Figure 1A) indicates that the base  
 250 peak (among peaks with the same DP) corresponds to the pseudo molecular ion [M+Na]<sup>+</sup> of the  
 251 fully methylated methylcellulose with methyl groups at both ends of the molecule, meaning that  
 252 both the C-1 hydroxyl of the glucosyl residue at the reducing end and the C-4 hydroxyl of the  
 253 glucosyl residue at the non-reducing end are methylated. The spectrum, however, also showed  
 254 peaks with lower intensities. For instance, sodium adduct ion peaks were found, corresponding to



255 tri-*O*-methyl cellulose (**1**) with a few non-methylated hydroxyl groups on the cellulosic backbone.  
256 Pseudo molecular ion  $[M+Na]^+$  peaks with  $m/z = 2313.760$  and  $2299.870$  were attributed to  
257 completely methylated methylcellulose ( $DP = 11$ ) and to methylcellulose ( $DP = 11$ ) with one  
258 hydroxyl group, respectively.



259  
260 **Figure 1.** MALDI-TOF MS spectra of (A) tri-*O*-methyl cellulose (**1**) ( $DP_n = 322$ ), (B) tri-*O*-methyl  
261 cellulosyl azide (**2**) ( $DP_n = 27.5$ ), and (C) propargyl tri-*O*-methyl celluloside (**3**) ( $DP_n = 13.2$ ).  
262

### 263 3.2. Synthesis of tri-*O*-methyl cellulosyl azide (**2**)

264 We tried to prepare the tri-*O*-methyl cellulosyl azide (**2**) using the synthetic strategy used for  
265 tri-*O*-acetyl- $\beta$ -cellulosyl azide (Kamitakahara, Enomoto, Hasegawa, & Nakatsubo, 2005). We  
266 have already found that the  $\alpha$ -anomer of acetyl tri-*O*-acetyl cellulose is relatively stable under  
267 azidation conditions using trimethylsilyl azide and  $SnCl_4$ . To replace the anomeric acetyl group  
268 with azide, a mixture of acetate  $\alpha$ - and  $\beta$ -anomers was first converted to the  $\beta$ -anomer of acetyl  
269 tri-*O*-acetyl cellulose via an  $S_N2$  reaction of tri-*O*-acetyl cellulosyl  $\alpha$ -bromide. The  $\beta$ -anomer of  
270 acetyl tri-*O*-acetyl cellulose was converted to tri-*O*-methyl  $\beta$ -cellulosyl azide. Hydrogen bromide,  
271 however, led to intensive degradation of tri-*O*-methyl cellulose (**1**), which was more reactive than  
272 tri-*O*-acetyl cellulose.

273

274 Due to the higher reactivity of tri-*O*-methyl cellulose (**1**) compared to tri-*O*-acetyl cellulose, we  
275 subsequently tried to prepare a mixture of  $\alpha$ - and  $\beta$ -anomers of tri-*O*-methyl cellulosyl azide (**2**)  
276 from  $\alpha$ - and  $\beta$ -anomers of methyl tri-*O*-methyl cellulose (**1**) in a one-step reaction. After the

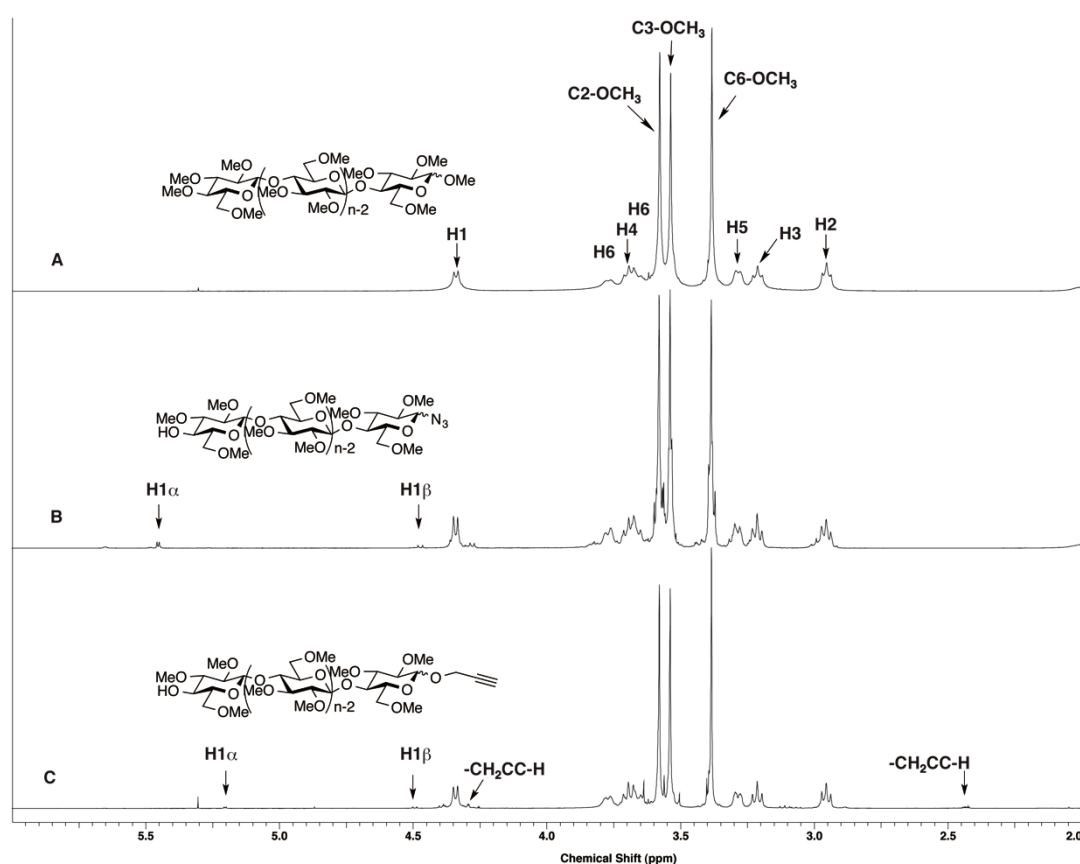
277 optimization of reaction conditions, the above synthesis was successfully accomplished.

278

279 The MALDI-TOF MS spectrum of tri-*O*-methyl cellulose azide (**2**) (Figure 1B) shows that it has  
280 one free hydroxyl group at the non-reducing end, specifically at the C-4 position of the glucosyl  
281 residue. The reaction mechanism to synthesis tri-*O*-methyl cellulose azide (**2**) having one free  
282 C-4 hydroxyl group attached to the glucosyl residue at the non-reducing end from tri-*O*-methyl  
283 cellulose (**1**) is illustrated in Scheme S1. Repetitive signals consisting of two major peaks are  
284 shown. For instance, pseudo molecular ion peaks with  $m/z = 2310.949$  ( $[M+Na]^+$ ) and  $m/z =$   
285  $2282.861$  ( $[M-N_2+Na]^+$ ) are attributed to tri-*O*-methyl cellulose azide (**2**) with  $DP = 11$  and one  
286 free hydroxyl group attached to the C-4 carbon of the glucosyl residue at the non-reducing end.

287

288 Figure 2 shows  $^1H$ -NMR spectra of tri-*O*-methyl cellulose (**1**), tri-*O*-methyl cellulose azide (**2**),  
289 and propargyl tri-*O*-methyl celloside (**3**). All proton resonances of tri-*O*-methyl cellulose (**1**)  
290 were assigned based on previous studies (Karakawa, Mikawa, Kamitakahara, & Nakatsubo, 2002;  
291 Nakagawa, Fenn, Koschella, Heinze, & Kamitakahara, 2011b). Resonances with low intensities at  
292 5.45 and 4.47 ppm were attributed to  $\alpha$ - and  $\beta$ -anomeric protons of the glucosyl residue at the  
293 reducing end of tri-*O*-methyl cellulose azide (**2**), respectively, as shown in Figure 2B.



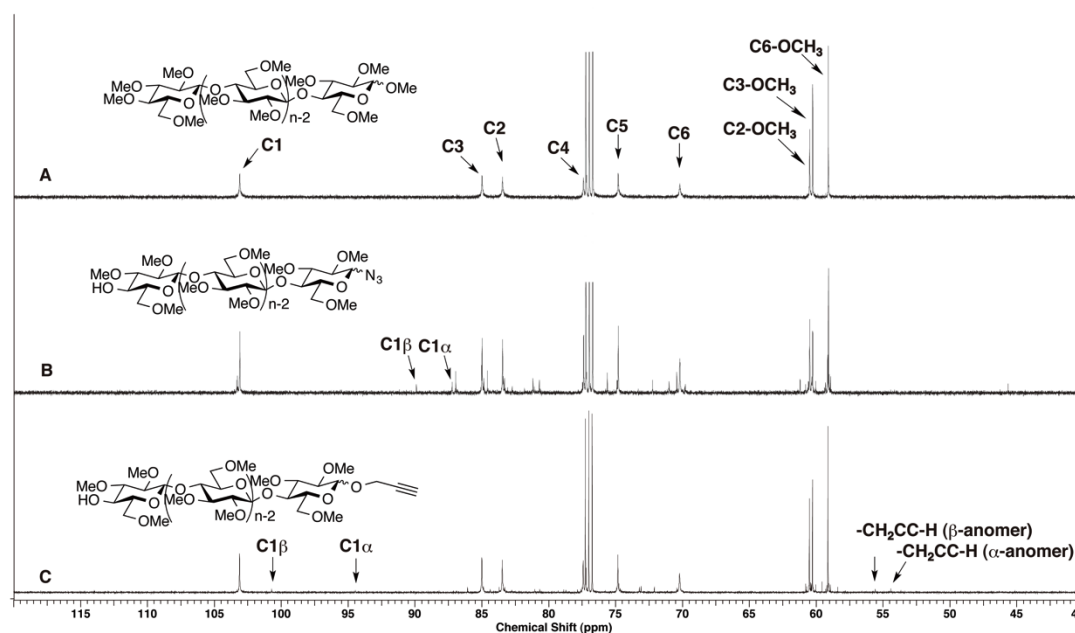
294

295 **Figure 2.**  $^1H$ -NMR spectra of (A) tri-*O*-methyl cellulose (**1**) ( $DP_n = 322$ ), (B) tri-*O*-methyl  
296 cellosyl azide (**2**) ( $DP_n = 27.5$ ), and (C) propargyl tri-*O*-methyl celloside (**3**) ( $DP_n = 71.2$ ).

297

298 All carbon resonances of tri-*O*-methyl cellulose (**1**) were also assigned, as shown in Figure 3. In  
299 Figure 3B, resonances with low intensities at 87.0 and 89.9 ppm were assigned to  $\alpha$ - and  
300  $\beta$ -anomeric carbons of the glucosyl residue at the reducing end of tri-*O*-methyl cellosyl azide (**2**),  
301 respectively.

302



303

304 **Figure 3.** <sup>13</sup>C-NMR spectra of (A) tri-*O*-methyl cellulose (**1**) ( $DP_n = 322$ ), (B) tri-*O*-methyl  
305 cellosyl azide (**2**) ( $DP_n = 27.5$ ), and (C) propargyl tri-*O*-methyl celloside (**3**) ( $DP_n = 71.2$ ).

306

### 307 3.3. Synthesis of propargyl tri-*O*-methyl celloside (**3**)

308 It was subsequently planned to prepare propargyl tri-*O*-methyl celloside (**3**) from tri-*O*-methyl  
309 cellulose (**1**) via in a one-step reaction. Propargyl alcohol was coupled at the C-1 position of the  
310 glucosyl residue at the reducing end of tri-*O*-methyl cellulose (**1**).

311 The MALDI-TOF MS spectrum of propargyl tri-*O*-methyl celloside (**3**) (Figure 1C) indicates that  
312 it has one free C-4 hydroxyl group attached to the glucosyl residue at the non-reducing end ( $DP_n =$   
313 13.2, obtained from tri-*O*-methyl cellulose having  $DP_n=65.4$ ), as exemplified by the detection of a  
314 pseudo molecular ion peak ( $[M+Na]^+$ ) with  $m/z = 2323.797$ . The expanded MALDI-TOF MS  
315 spectra are shown in Figure S1. The reaction mechanism to synthesis propargyl tri-*O*-methyl  
316 celloside (**3**) having one free C-4 hydroxyl group attached to the glucosyl residue at the  
317 non-reducing end from tri-*O*-methyl cellulose (**1**) is illustrated in Scheme S1.

318

319 As shown in Figure 2C, the <sup>1</sup>H-NMR spectrum of propargyl tri-*O*-methyl celloside (**3**) showed  
320 signals of alkyne and methylene protons of the propargyl group at 2.43 and 4.28–4.39 ppm,

321 respectively. In the corresponding  $^{13}\text{C}$ -NMR spectrum (Figure 3C), the methylene carbons of the  
322 propargyl group appeared at 54.4 ( $\underline{\text{C}}\text{H}_2\text{CCH}$  (C1- $\alpha$ )) and 55.6 ppm ( $\underline{\text{C}}\text{H}_2\text{CCH}$  (C1- $\beta$ )). Anomeric  
323 protons of the glucosyl residue at the reducing end of propargyl tri-*O*-methyl cellulose (**3**)  
324 appeared at 4.49 (H1- $\beta$ ) and 5.20 ppm (H1- $\alpha$ ), as shown in Figure 2C. In addition, anomeric  
325 carbons of the glucosyl residue at the reducing end of propargyl tri-*O*-methyl cellulose (**3**)  
326 appeared at 94.5 (C1- $\alpha$ ) and 100.7 ppm (C1- $\beta$ ), as shown in Figure 3C.

327

### 328 **3.4. Control of molecular weight of cellulose ethers carrying two independent end-functional** 329 **groups**

330 The molecular weight of end-functionalized cellulose ethers influences the physical properties of  
331 block copolymers when they are used as one of the molecular Lego bricks. For instance, a  
332 well-defined diblock copolymer exhibits microphase separation (Kamitakahara, Baba, Yoshinaga,  
333 Suhara, & Takano, 2014), which has received considerable attention. Molecular lengths of the two  
334 segments usually affect microphase separation patterns of diblock copolymers, motivating us to  
335 explore reaction conditions for obtaining end-functionalized cellulose ethers with tailored molecular  
336 weights.

337 End-azidation of tri-*O*-methyl cellulose (**1**) was carried out with trimethylsilyl azide and  $\text{SnCl}_4$  in  
338 anhydrous chloroform, with reaction conditions summarized in Table 1. The degree of  
339 polymerization of tri-*O*-methyl cellulose azide (**2**) decreased with increasing amounts of  $\text{SnCl}_4$ .  
340 This result means that we are able to control the DP of tri-*O*-methyl cellulose azide (**2**). Actually,  
341 tri-*O*-methyl cellulose azide (**2**) having one free C-4 hydroxyl group attached to the glucosyl  
342 residue at the non-reducing end with DP from 20 to 81 was produced.

343

344 **Table 1.** Azido end-functionalization of tri-*O*-methyl cellulose (**1**).

entry	TMS- $\text{N}_3$ (equiv/AGU)	$\text{SnCl}_4$ (equiv./AGU)	$M_n/10^4$	$M_w/M_n$	$DP_n$
1	0.195	0.034	1.7	2.0	81
2	0.390	0.067	1.1	1.9	54
3	0.585	0.100	0.41	2.9	20

345

346

347 Moreover, end-propargylation of tri-*O*-methyl cellulose (**1**) was carried out with 2-propyne-1-ol and  
348  $\text{SnCl}_4$  in anhydrous dichloromethane, with reaction conditions summarized in Table 2. The DP of  
349 propargyl tri-*O*-methyl cellulose (**3**) decreased with increasing amounts of  $\text{SnCl}_4$ . This result  
350 means that we are also able to control the DP of propargyl tri-*O*-methyl cellulose (**3**) having one  
351 free C-4 hydroxyl group attached to the glucosyl residue at the non-reducing end, producing the  
352 above compound with DP from 29 to 45.

353

354 **Table 2.** Propargyl end-functionalization of tri-*O*-methyl cellulose (**1**).

entry	2-propyn-1-ol (equiv./AGU)	SnCl <sub>4</sub> (equiv./AGU)	$M_n/10^3$	$M_w/M_n$	$DP_n$
1	0.3	0.070	9.2	1.9	45
2	0.3	0.085	7.7	2.2	38
3	0.3	0.100	6.0	2.0	29

355

356

357 **4. Conclusion**

358 MALDI-TOF MS, <sup>1</sup>H- and <sup>13</sup>C-NMR spectra confirm that the end-functionalization of fully  
 359 methylated cellulose proceeded to afford cellulosic molecular rods carrying two independent end  
 360 groups at the both ends of the molecules. Controlled degradation of the fully protected cellulose  
 361 ethers by Lewis acid in presence of trimethylsilyl azide or propargyl alcohol produced tri-*O*-methyl  
 362 cellulosyl azide (**2**) and propargyl tri-*O*-methyl cellulose (**3**) with tailored DP, respectively, having  
 363 a free hydroxyl group at the C-4 position of the non-reducing glucopyranosyl residue. These  
 364 methods furnished end-functionalized cellulose ethers as semi-rigid linear hydrophobic molecular  
 365 Lego bricks with tunable degrees of polymerization. The free C-4 hydroxyl of the glucosyl  
 366 residue at the non-reducing end could connect with other molecular bricks, thereby extending the  
 367 variety of molecular architecture motifs. The developed chemistry will enable us to initiate a new  
 368 era of precise block architecture of polysaccharide derivatives.

369

370 **Acknowledgements**

371 We thank the Japan Society for the Promotion of Science (JSPS) for their financial support of this  
 372 study, in part through Grant-in-Aid for Scientific Research (Nos. 24380092 and 15H04531).

373

374 **Supporting Information**

375 Reaction mechanisms of the tri-*O*-methyl cellulosyl azide (**2**) and propargyl tri-*O*-methyl  
 376 cellulose (**3**) syntheses from tri-*O*-methyl cellulose (**1**) are illustrated in Scheme S1.  
 377 MALDI-TOF MS spectra of tri-*O*-methyl cellulose (**1**), tri-*O*-methyl cellulosyl azide (**2**), and  
 378 propargyl tri-*O*-methyl cellulose (**3**) in the region of  $DP = 11$  are shown in Figure S1.  
 379 MALDI-TOF MS spectra of tri-*O*-methyl cellulose (**1**) with a  $DP_n$  of 322, obtained using positive  
 380 ion linear mode, are shown in Figure S2. Expanded <sup>1</sup>H- and <sup>13</sup>C-NMR spectra of tri-*O*-methyl  
 381 cellulose (**1**) ( $DP_n = 322$ ), tri-*O*-methyl cellulosyl azide (**2**) ( $DP_n = 27.5$ ), and propargyl  
 382 tri-*O*-methyl cellulose (**3**) ( $DP_n = 71.2$ ) in the anomeric proton region are shown in Figures S3  
 383 and S4, respectively.

384

385 **References**

- 386 De Oliveira, W., & Glasser, W. G. (1994). Novel cellulose derivatives. II. Synthesis and  
387 characteristics of mono-functional cellulose propionate segments. *Cellulose*, *1*, 77-86.
- 388 Enomoto, Y., Kamitakahara, H., Takano, T., & Nakatsubo, F. (2006). Synthesis of diblock  
389 copolymers with cellulose derivatives. 3. Cellulose derivatives carrying a single pyrene group  
390 at the reducing-end and fluorescent studies of their self-assembly systems in aqueous NaOH  
391 solutions. *Cellulose*, *13*(4), 437-448.
- 392 Enomoto-Rogers, Y., Kamitakahara, H., Yoshinaga, A., & Takano, T. (2010). Radially oriented  
393 cellulose triacetate chains on gold nanoparticles. *Cellulose*, *17*(5), 923-936.
- 394 Enomoto-Rogers, Y., Kamitakahara, H., Yoshinaga, A., & Takano, T. (2012). Comb-shaped graft  
395 copolymers with cellulose side-chains prepared via click chemistry. *Carbohydrate Polymers*,  
396 *87*(3), 2237-2245.
- 397 Kamitakahara, H., Baba, A., Yoshinaga, A., Suhara, R., & Takano, T. (2014). Synthesis and  
398 crystallization-induced microphase separation of cellulose  
399 triacetate-block-poly( $\gamma$ -benzyl-L-glutamate). *Cellulose*, *21*, 3323-3338.
- 400 Kamitakahara, H., Enomoto, Y., Hasegawa, C., & Nakatsubo, F. (2005). Synthesis of diblock  
401 copolymers with cellulose derivatives. 2. Characterization and thermal properties of cellulose  
402 triacetate-*block*-oligoamide-15. *Cellulose*, *12*(5), 527-541.
- 403 Kamitakahara, H., Hori, M., & Nakatsubo, F. (1996). Substituent effect on ring-opening  
404 polymerization of regioselectively acylated  $\alpha$ -D-glucopyranose 1,2,4-orthopivalate derivatives.  
405 *Macromolecules*, *29*(19), 6126-6131.
- 406 Kamitakahara, H., Koschella, A., Mikawa, Y., Nakatsubo, F., Heinze, T., & Klemm, D. (2008).  
407 Syntheses and comparison of 2,6-di-*O*-methyl celluloses from natural and synthetic celluloses.  
408 *Macromolecular Bioscience*, *8*(7), 690-700.
- 409 Kamitakahara, H., & Nakatsubo, F. (2005). Synthesis of diblock copolymers with cellulose  
410 derivatives. 1. Model study with azidoalkyl carboxylic acid and cellobiosylamine derivative.  
411 *Cellulose*, *12*(2), 209-219.
- 412 Karakawa, M., Mikawa, Y., Kamitakahara, H., & Nakatsubo, F. (2002). Preparations of  
413 regioselectively methylated cellulose acetates and their H-1 and C-13 NMR spectroscopic  
414 analyses. *Journal of Polymer Science Part A-Polymer Chemistry*, *40*(23), 4167-4179.
- 415 Kim, S., Stannett, V. T., & Gilbert, R. D. (1973). A new class of biodegradable polymers. *Journal of*  
416 *Polymer Science Polymer Letters Edition*, *11*, 731-735.
- 417 Kim, S., Stannett, V. T., & Gilbert, R. D. (1976). Biodegradable Cellulose Block Copolymers.  
418 *Journal of Macromolecular Science. Pt. A, Chemistry*, *A10*(4), 671-679.
- 419 Kolb, H. C., Finn, M. G., & Sharpless, K. B. (2001). Click chemistry: diverse chemical function  
420 from a few good reactions. *Angew. Chem., Int. Ed.*, *40*, 2004-2021.

421 Lepage, M. L., Schneider, J. P., Bodlenner, A., & Compain, P. (2015). Toward a Molecular Lego  
422 Approach for the Diversity-Oriented Synthesis of Cyclodextrin Analogues Designed as  
423 Scaffolds for Multivalent Systems. *J. Org. Chem.*, *80*, 10719-10733.

424 Meldal, M. (2008). Polymer "clicking" by CuAAC reactions. *Macromol. Rapid Commun.*, *29*,  
425 1016-1051.

426 Nakagawa, A., Fenn, D., Koschella, A., Heinze, T., & Kamitakahara, H. (2011a). Physical  
427 Properties of Diblock Methylcellulose Derivatives with Regioselective Functionalization  
428 Patterns: First Direct Evidence that a Sequence of 2,3,6-Tri-*O*-methyl-glucoopyranosyl Units  
429 Causes Thermoreversible Gelation of Methylcellulose. *Journal of Polymer Science Part*  
430 *B-Polymer Physics*, *49*(21), 1539-1546.

431 Nakagawa, A., Fenn, D., Koschella, A., Heinze, T., & Kamitakahara, H. (2011b). Synthesis of  
432 Diblock Methylcellulose Derivatives with Regioselective Functionalization Patterns. *Journal of*  
433 *Polymer Science Part A-Polymer Chemistry*, *49*(23), 4964-4976.

434 Nakagawa, A., Ishizu, C., Sarbova, V., Koschella, A., Takano, T., Heinze, T., & Kamitakahara, H.  
435 (2012). 2-*O*-Methyl- and 3,6-Di-*O*-methyl-cellulose from Natural Cellulose: Synthesis and  
436 Structure Characterization. *Biomacromolecules*, *13*(9), 2760-2768.

437 Nakagawa, A., Kamitakahara, H., & Takano, T. (2011). Synthesis of blockwise alkylated (1-->4)  
438 linked trisaccharides as surfactants: influence of configuration of anomeric position on their  
439 surface activities. *Carbohydr Res*, *346*(13), 1671-1683.

440 Nakagawa, A., Kamitakahara, H., & Takano, T. (2012). Synthesis and thermoreversible gelation of  
441 diblock methylcellulose analogues via Huisgen 1,3-dipolar cycloaddition. *Cellulose*, *19*(4),  
442 1315-1326.

443 Nakagawa, A., Steiniger, F., Richter, W., Koschella, A., Heinze, T., & Kamitakahara, H. (2012).  
444 Thermoresponsive Hydrogel of Diblock Methylcellulose: Formation of Ribbonlike  
445 Supramolecular Nanostructures by Self-Assembly. *Langmuir*, *28*(34), 12609-12618.

446 Nakatsubo, F., Kamitakahara, H., & Hori, M. (1996). Cationic ring-opening polymerization of  
447 3,6-di-*O*-benzyl- $\alpha$ -D-glucose 1,2,4-orthopivalate and the first chemical synthesis of cellulose.  
448 *Journal of the American Chemical Society*, *118*(7), 1677-1681.

449 Pohjola, L., & Eklund, V. (1977). Polyurethane block copolymers from cellulose acetate. *Paperi ja*  
450 *Puu*, *3*, 117-120.

451 Savage, A. B. (1957). Temperature-Viscosity Relationships for Water-Soluble Cellulose Ethers.  
452 *Industrial and Engineering Chemistry*, *49*, 99.

453 Steinmann, H. W. (1968). Novel cellulose and segmented copolymers. (p. 17 pp.): Celanese  
454 Corp. .

455 Steinmann, H. W. (1970). Elastomeric fibers from cellulose acetate. *Polym. Prepr., Am. Chem. Soc.*  
456 *Div. Polym. Chem.*, *11*(1), 285-290.

457

458

459 **Figure Captions**

460 **Scheme 1.** Synthesis of tri-*O*-methyl cellulosyl azide (**2**) and propargyl tri-*O*-methyl celluloside (**3**)  
461 from tri-*O*-methyl cellulose (**1**).

462 **Figure 1.** MALDI-TOF MS spectra of (A) tri-*O*-methyl cellulose (**1**) ( $DP_n = 322$ ), (B) tri-*O*-methyl  
463 cellulosyl azide (**2**) ( $DP_n = 27.5$ ), and (C) propargyl tri-*O*-methyl celluloside (**3**) ( $DP_n = 13.2$ ).

464 **Figure 2.**  $^1\text{H-NMR}$  spectra of (A) tri-*O*-methyl cellulose (**1**) ( $DP_n = 322$ ), (B) tri-*O*-methyl  
465 cellulosyl azide (**2**) ( $DP_n = 27.5$ ), and (C) propargyl tri-*O*-methyl celluloside (**3**) ( $DP_n = 71.2$ ).

466 **Figure 3.**  $^{13}\text{C-NMR}$  spectra of (A) tri-*O*-methyl cellulose (**1**) ( $DP_n = 322$ ), (B)  
467 tri-*O*-methylcellulosyl azide (**2**) ( $DP_n = 27.5$ ), and (C) propargyl tri-*O*-methyl celluloside (**3**) ( $DP_n$   
468 = 71.2).

469

470 **Table 1.** Azido end-functionalization of tri-*O*-methyl cellulose (**1**).

471 **Table 2.** Propargyl end-functionalization of tri-*O*-methyl cellulose (**1**).